Temperature dependence of the local structure around the tantalum atom in potassium tantalate

1994 J. Phys.: Condens. Matter 6 9317

(http://iopscience.iop.org/0953-8984/6/44/012)

J. Phys.: Condens. Matter 6 (1994) 9317–9328. Printed in the UK

Temperature dependence of the local structure around the tantalum atom in potassium tantalate

Y Nishihata†, O Kamishima†, K Ojima†, A Sawada†, H Maeda† and H Terauchi‡

† Faculty of Science, Okayama University, Okayama 700, Japan
‡ School of Science, Kwansei Gakuin University, Nishinomiya 662, Japan

Received 22 February 1994, in final form 7 June 1994

Abstract. The local structure around the Ta atom in potassium tantalate $KTaO_3$ has been investigated using extended x-ray absorption fine-structure (EXAFS) measurements. EXAFS spectra near the Ta L_{III} edge were observed at 24, 40, 100, 150, 200, 250 and 298 K. The Debye–Waller factor has been analysed in detail as also have other local structure parameters. Anharmonicity of the thermal vibration of the Ta atom which is located at the centre of an oxygen octahedron is almost negligible below room temperature, while anisotropy of the thermal vibration of the Ta atom increases gradually with decreasing temperature. It has been found that the anisotropic thermal vibration in the ⟨001⟩ directions at low temperatures, which was estimated by EXAFS analysis, corresponds to the softening of the transverse optical phonon at the Brillouin zone centre found by an inelastic neutron scattering study.

1. Introduction

Many cubic perovskite crystals undergo phase transitions, where they transform to slightly distorted structures from the ideal perovskite structure. The condensation of a phonon mode which was predicted by Cochran [1] is a useful concept to explain the successive phase transitions of perovskite crystals such as $SrTiO_3$, $BaTiO_3$ and $PbTiO_3$ [2–6]. However, overdamping of the soft phonon mode and a central peak were observed in some cases and suggest that these phase transitions cannot be regarded simply as of displacive type [7–9]. On the other hand, Comes *et al* [10] measured x-ray diffuse scattering and proposed a model in which there must be a linear disorder of atoms in $KTaO_3$ as well as in the other perovskite crystals, such as $BaTiO_3$, $KNbO_3$, $NaNbO_3$ and $KMnF_3$ [11–14]. Recently, structure refinements obtained by a diffraction study on some perovskites of single crystals suggest the disorder of atoms. Itoh *et al* [15] reported that the Ti atom in $BaTiO_3$ shifts from the centre of the O octahedron in the ⟨111⟩ directions in the cubic phase, while the Ti atom in $SrTiO_3$ is located at the centrosymmetric position. Nelmes *et al* [16] also reported disorder of the Pb atom in $PbTiO_3$ even above the Curie temperature, although this crystal has been regarded as a typical ferroelectric which undergoes a displacive-type phase transition. In the confusing situation about the mechanism of the phase transitions of the perovskites, the purpose of this work is to study local structures of perovskites near the phase transitons to determine the origin of the overdamping of the phonon mode and a central peak by studying local structures using the extended x-ray absorption fine-structure (EXAFS) technique. Recently a shift of the Nb atom in $KNbO_3$ from the central position along ⟨111⟩ axes was found through an EXAFS study by de Mathan *et al* [17]. The disorder of the Ti

0953-8984/94/449317+12$19.50

atom in $PbTiO_3$ in the cubic phase was suggested from EXAFS and x-ray absorption near-edge structure (XANES) studies by Ravel *et al* [18]. We are also interested in the temperature dependence of the Debye–Waller factor in the EXAFS function on the crystals in which the soft phonon mode was found.

In $KTaO_3$, no phase transition occurs and it is regarded as a quantum paraelectric because long-range ordering of the dipole moments is suppressed by the quantum fluctuation at very low temperatures [19–22]. Shirane and co-workers [23–25] found softening of the transverse optical phonon at the Brillouin zone centre along the [001] direction by inelastic neutron scattering studies. This phonon mode is well defined and not overdamped. They reported that the anomalous temperature dependence of the dielectric constant, which deviated from the simple Curie–Weiss law at both low and high temperatures, is faithfully reflected in the temperature dependence of the soft mode. Later, the temperature dependence of the dielectric constant was explained by several workers [19–22] using an expression which considers quantum effects and which was derived by Barrett [26]. Comes and Shirane [25] concluded that the linear correlation of the atomic displacement along the ⟨001⟩ directions is dynamic. The strong dynamic correlation within a Ta–O chain is consistent with the x-ray diffuse scattering in the {100} reciprocal sheets. In the low-temperature range, we can expect short-range ordering or a local structure modification as an incipient ferroelectric.

In this paper, we deal with Debye–Waller factors of the Ta–O atomic pair in detail and discuss the temperature dependence of anisotropic thermal vibration of the Ta atom in $KTaO_3$.

2. Experiment

The purity of the $KTaO_3$ investigated was 99.9%. The sample was confirmed in advance to have the cubic perovskite structure by an x-ray powder diffraction profile. The powder sample was dusted onto Scotch tape and held between Al foils to keep the temperature uniform. X-ray absorption spectra were measured using an EXAFS facility installed at the beam line 10B of the 2.5 GeV storage ring of the Photon Factory in the National Laboratory of High Energy Physics (Tsukuba). Measurements were carried out in transmission mode with a Si(311) channel cut monochromator. The incident and transmitted x-ray intensities were monitored with an ionization chamber 17 cm long with flowing N_2 gas and an ionization chamber 31 cm long with flowing N_2–15% Ar gas, respectively. The photon energy E was calibrated with a Cu foil by assigning 8.9788 keV to the pre-edge peak of the absorption. The temperature of the sample was controlled with a closed-cycle He-gas refrigerator. EXAFS spectra near the Ta L_{III} edge of $KTaO_3$ were obtained at 24, 40, 100, 150, 200, 250 and 298 K.

3. Analysis

Figure 1 shows the x-ray absorption spectrum $\mu(E)d$ near the Ta L_{III} edge of $KTaO_3$ at 24 K as an example. Here d is the sample thickness. A well defined EXAFS signal is found up to the Ta L_{II} edge. The Victoreen function fitted is also shown in this figure. The EXAFS function $\chi(k)$ was extracted from the absorption spectrum following the standard procedure [27]. Here the $\chi(k)$ was normalized using MacMaster coefficients according to the EXAFS

workshop report [28]. The programs XAFS93 and MBF93 were employed for the EXAFS data analyses. The Fourier transform of $\chi(k)$ yields a radial structure function $\phi(R)$:

$$\phi(R) = \frac{1}{\sqrt{2\pi}} \int_{k_{min}}^{k_{max}} w(k) k^n \chi(k) \exp(2ikR)\, dk \tag{1}$$

where $w(k)$ is a Hanning window function and k^n with $n = 3$ is a k-weighting term to compensate for diminishing amplitudes at high k-values. Here the wavenumber of a photoelectron is represented as $k = [2m(E - E_0)/\hbar^2]^{1/2}$, where m and $\hbar$ are the mass of the electron and Planck's constant, respectively. The threshold energy E_0 was assigned to an inflection point of the absorption edge. Figure 2 shows radial structure functions $\phi(R)$ around the Ta atom at 24 and 298 K obtained by a Fourier transform of $k^3\chi(k)$ in the range 3.4 $Å^{-1} \leqslant k \leqslant 17.5$ $Å^{-1}$. The correction of the phase shift is not taken into account at this stage. We can assign the peak in $\phi(R)$ to the first-nearest-neighbour O atom from the crystallographic value obtained by the diffraction data; the distance between the Ta and O atoms is 1.9942(1) Å [20].

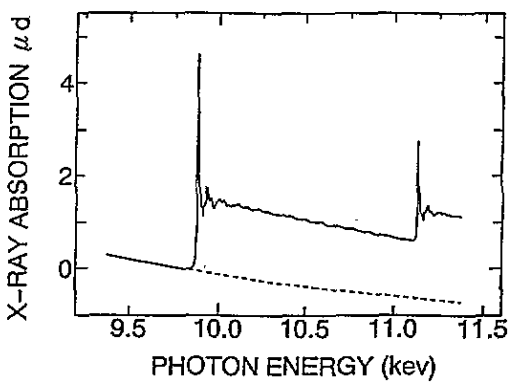

Figure 1. X-ray absorption spectrum near the Ta L_{III} edge of $KTaO_3$ at 24 K: ----, the Victoreen function.

In order to determine the local structure parameters taking account of an anharmonic thermal vibration, we used an EXAFS formula based on the single-scattering theory and expressed by the cumulant expansion up to the fourth-order term [29]:

$$\chi(k) = \sum_j \frac{N_j}{kR_j^2} |f_j(k;\pi)| \exp(-2\sigma_j^{(2)}k^2 + \tfrac{2}{3}\sigma_j^{(4)}k^4) \exp\left(-\frac{2R_j}{\lambda_j}\right) \times \sin\left[2kR_j - \frac{2k}{R_j}\left(1 + \frac{2R_j}{\lambda_j}\right)\sigma_j^{(2)} - \tfrac{4}{3}\sigma_j^{(3)}k^3 + \psi_j(k)\right] \tag{2}$$

where N_j is the coordination number in the jth shell at distance R_j from the absorbing atom, $|f_j(k;\pi)|$ the back-scattering amplitude of photoelectrons and $\psi_j(k)$ the total phase shift function. Values of the functions $|f_j(k;\pi)|$ and $\psi_j(k)$ were taken from the theoretical table of Mckale *et al* [30]. The quantities $\sigma_j^{(n)}$ are the nth cumulants. The mean free path λ_j of the photoelectron was supposed to depend on the wavevector k : $\lambda_j = k/\eta_j$. When we accept a harmonic vibration model, the quantities $\sigma^{(3)}$ and $\sigma^{(4)}$ must be zero.

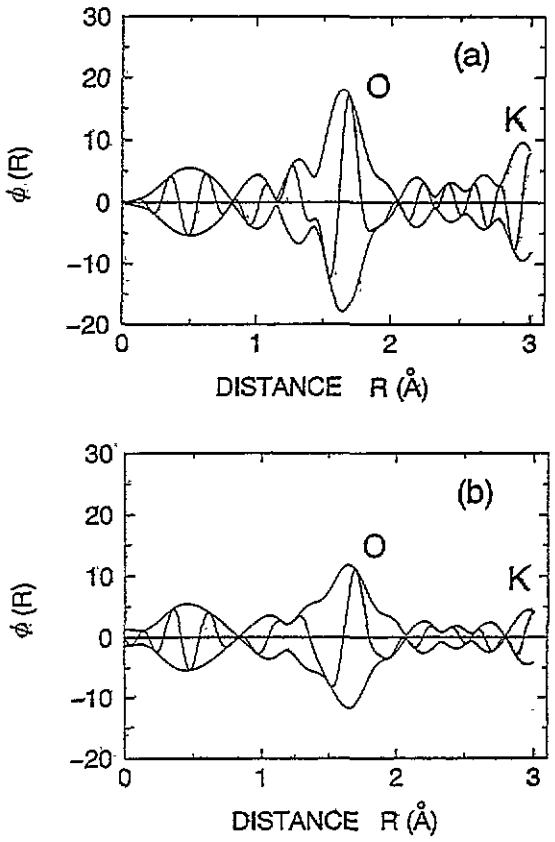

Figure 2. Radial structure functions $\phi(R)$ (magnitude and imaginary part of Fourier transform of the EXAFS oscillations) around the Ta atom: (*a*) 24 K; (*b*) 298 K.

In the parameter fitting, according to the EXAFS workshop report [28], we filtered a theoretical EXAFS function the same way as the observed function to eliminate truncation effects through the Fourier transformation of the data. We use a non-linear least-squares fitting method to determine the local structure parameters. The equal deformation of observed and theoretical EXAFS functions improves the accuracy of the parameter fitting. This technique enables us to narrow down the region of Fourier transform in the real space. We can choose the range of Fourier transform to exclude the influence from the atoms except the interested atom and ghost peaks near the origin (the absorbing atom) in the real space. Moreover, we can make use of a wide range in the k-space since we need not abandon the marginal region which was distorted by the window function.

The discrepancy factor (R-factor) between the theoretical and experimental EXAFS functions χ_{calc} and χ_{obs} is defined as follows:

$$R = \sum_k [k^n \chi_{obs}(k) - k^n \chi_{calc}(k)]^2 \Big/ \sum_k [k^n \chi_{obs}(k)]^2. \tag{3}$$

In general, the R-factor estimated by the technique of Fourier filtering theoretical EXAFS function twice is about one order of magnitude smaller than that estimated by the conventional method [31]. It seems that a Debye–Waller-type factor is worth discussing in detail by this technique.

4. Results and discussion

4.1. Harmonicity of atomic vibration (one-shell model)

The Fourier-filtered EXAFS function was obtained by the Fourier transform of the O peak in the range 1.2 Å $\leqslant R \leqslant$ 2.1 Å. The fitting analysis was carried out by comparing the observed and theoretical EXAFS functions in the range 3.5 $Å^{-1} \leqslant k \leqslant 11.2$ $Å^{-1}$. First of all, we assumed that the Ta atom is located at the centre of the O octahedron. The number of O atoms was fixed to six. Table 1 gives local structure parameters of the O shell around the Ta atom. The interatomic distance R_{Ta-O} between the Ta and O atoms is in good agreement with the value determined by x-ray diffraction within a deviation of about 0.01 Å. The thermal expansion of $KTaO_3$ is very small. The reduction in the lattice constant of $KTaO_3$ from 298 to 8 K is about 0.004 Å [20] and almost corresponds to the estimated standard deviation of the interatomic distance R_{Ta-O}. It can be regarded as a constant value below room temperature in the EXAFS analysis. The parameters η and ΔE_0 are found to be not dependent on temperature. Here ΔE_0 is the difference between the theoretical and the experimental threshold energies. The least-squares fittings converged at small R-factors. Figure 3 shows the Debye–Waller factor $\sigma^{(2)}$ between the Ta and O atoms as a function of temperature. An increase in $\sigma^{(2)}$ was expected in the low-temperature region, which will correspond to the anomalous temperature dependence of the dielectric constant or the softening of the ferroelectric phonon mode, but $\sigma^{(2)}$ decreases with decreasing temperature as seen in the figure. In the EXAFS technique, we can obtain knowledge about the relative distance and the relative atomic motion between the absorbing and surrounding atoms. The Debye–Waller factor in the EXAFS function contains information concerning all modes of atomic vibration. It seems that the contribution of a soft mode to $\sigma^{(2)}$ will smear out in the one-shell model when we consider local structures. Then we examined anharmonicity of atomic vibration in the data obtained at 24 and 298 K. The number of nearest-neighbour O atoms was also fixed to six. The cumulant $\sigma^{(3)}$ which referred to an asymmetric atomic motion was constrained to be zero because the Ta atom is located at the inversion centre. Other parameters are listed in table 2. In the calculation, the correlation between the parameters was considered carefully. The higher-order cumulant $\sigma^{(4)}$ is almost zero in comparison with the estimated standard deviation at both temperatures. This indicates that the thermal vibration between the Ta and O atoms does not have anharmonicity below room temperature. As a result of the parameter fitting of one-shell models, the anharmonicity of atomic vibration is so small that we need not introduce disorder of the Ta atom in further analysis.

Table 1. Local structure parameters of the O shell around the Ta atom for the harmonic vibration model (one-shell model). The coordination number N of the O atom was fixed at 6.

Temperature (K)	N	R_{Ta-O} (Å)	$\sigma^{(2)}$ ($Å^2$)	η ($Å^{-2}$)	ΔE_0 (keV)	R-factor (%)
24	6	2.008(1)	0.0046(2)	0.66(2)	0.0171(3)	1.6
40	6	2.007(1)	0.0047(2)	0.67(2)	0.0169(3)	1.9
100	6	2.006(1)	0.0053(2)	0.68(2)	0.0164(3)	5.1
150	6	2.001(1)	0.0059(2)	0.64(2)	0.0162(3)	3.8
200	6	2.006(1)	0.0058(2)	0.71(3)	0.0165(3)	3.5
250	6	2.007(2)	0.0068(2)	0.66(3)	0.0170(3)	1.5
298	6	2.005(2)	0.0070(2)	0.69(3)	0.0163(3)	3.9

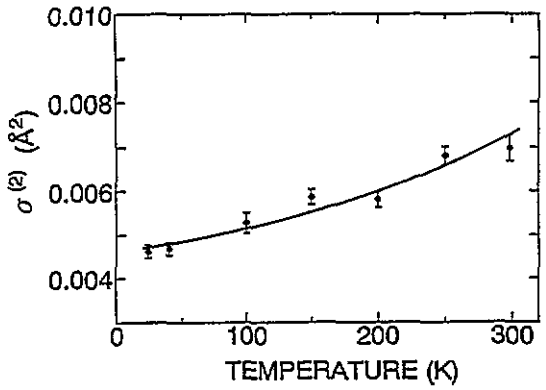

Figure 3. Temperature dependence of the Debye–Waller factor $\sigma^{(2)}$ on the Ta–O atomic pair for the one-shell model: ——, guide to the eye.

Table 2. Local structure parameters of the O shell around the Ta atom for the anharmonic vibration model (one-shell model). The coordination number N of the O atom was fixed at 6. The cumulant $\sigma^{(3)}$ was fixed at 0 owing to the centre of symmetry.

Temperature (K)	N	R_{Ta-O} (Å)	$\sigma^{(2)}$ (Å^2)	$\sigma^{(3)}$ (Å^3)	$\sigma^{(4)}$ (Å^4)	η (Å^{-2})	ΔE_0 (keV)	R-factor (%)
24	6	2.008(1)	0.0049(2)	0	0.000 008(6)	0.65(2)	0.0172(3)	1.6
298	6	2.005(2)	0.0070(2)	0	0.000 000(9)	0.69(3)	0.0163(3)	3.9

A slight softening of the transverse acoustic phonon mode due to the coupling of the transverse and optic phonon modes was reported at low temperatures by Axe *et al* [24]. Fujikawa and Miyanaga [32] have studied the contribution from optical and acoustic phonon modes to the Debye–Waller factor in the EXAFS function on the basis of quantum statistics. In EXAFS analysis we cannot recognize the q-dependence of a phonon mode. However, the contribution of an optical phonon to the Debye–Waller factor in the EXAFS function is larger than that of an acoustic phonon because the atomic displacement of the optical phonon mode is relatively larger, and the excitation of an acoustic mode is not sufficient at low temperatures. This suggests that the transverse optical phonon does not have anharmonicity at low temperatures, although we cannot estimate quantitatively the contribution from acoustic phonon modes. The harmonicity of atomic vibration observed by EXAFS implies that the coupling of optical and acoustic phonon modes is important to understand the softening of phonon mode in this crystal as pointed out by Chaves *et al* [22].

4.2. Anisotropy of atomic vibration (two-shell model)

Harada *et al* [33] carried out a mode analysis of this crystal at room temperature by an inelastic neutron scattering study. The mode was identified as being of the Slater type. In the Slater mode, the Ta atom vibrates against the O octahedron; the Ta and O atoms vibrate in the axial direction in the opposite phase. The difference between the thermal vibration in the axial direction and that in the equatorial plane implies an anisotropic thermal vibration of the Ta atom. In the next stage, we considered a two-shell model with two different Debye–Waller factors, while the Ta atom is still located at the centre of the O octahedron.

In general, the EXAFS function $\chi(k)$ for one shell is divided into two parts [34]:

$$\chi(k) = 6\chi_0(k)\langle G(\delta u)\rangle \tag{4}$$

where $\chi_0(k)$ is an EXAFS function for one O atom without considering thermal vibrations and $\langle G(\delta u)\rangle$ represents a damping factor which depends on the relative atomic displacement δu. The damping factor is averaged with respect to the dynamic disorder which arises from the thermal vibration of atoms. The EXAFS function $\chi(k)$ contains the contribution from two O atoms which vibrate in the axial direction and four O atoms which vibrate in the equatorial plane:

$$\chi(k) = 2\chi_0(k)\langle G(\delta u)\rangle_{ax} + 4\chi_0(k)\langle G(\delta u)\rangle_{eq}. \tag{5}$$

Table 3 gives the local structure parameters of the O shell around the Ta atom for the two-shell model. The parameters R_{Ta-O}, η and ΔE_0 were constrained to have the same values for both shells. Consequently, they agree with the values obtained from the one-shell model within the estimated standard deviation. The least-squares fittings converged at almost the same R-factors as the one-shell model. Figure 4 shows the temperature dependence of the two Debye–Waller factors $\sigma_{ax}^{(2)}$ and $\sigma_{eq}^{(2)}$, where they correspond to the Debye–Waller factors in the axial direction and the equatorial plane, respectively. $\sigma_{eq}^{(2)}$ decreases with decreasing temperature, while the $\sigma_{ax}^{(2)}$ maintains an almost constant value from 298 to 24 K. As shown in figure 5, the theoretical value of $k^3\chi(k)$ agrees excellently with the experimental value.

Table 3. Local structure parameters of O shells around the Ta atom for the harmonic vibration model (two-shell model). The coordination numbers N of the O atom were fixed at 2 and 4 for each O shell. The parameters R_{Ta-O}, η and ΔE_0 were calculated as the same values for each O shell.

Temperature (K)	N	R_{Ta-O} (Å)	$\sigma_{ax}^{(2)}$ (Å^2)	$\sigma_{eq}^{(2)}$ (Å^2)	η (Å^{-2})	ΔE_0 (keV)	R-factor (%)
24	2 4	2.008(1)	0.0072(6)	0.0037(2)	0.65(2)	0.0172(3)	1.6
40	2 4	2.007(1)	0.0069(6)	0.0039(2)	0.66(2)	0.0169(3)	1.9
100	2 4	2.005(1)	0.0084(8)	0.0042(2)	0.66(3)	0.0164(3)	5.1
150	2 4	2.001(1)	0.0073(6)	0.0053(2)	0.64(2)	0.0162(3)	3.8
200	2 4	2.006(1)	0.0072(7)	0.0052(3)	0.71(3)	0.0165(3)	3.5
250	2 4	2.007(2)	0.0073(7)	0.0066(3)	0.66(3)	0.0170(3)	1.5
298	2 4	2.005(2)	0.0068(6)	0.0070(3)	0.69(3)	0.0163(3)	3.9

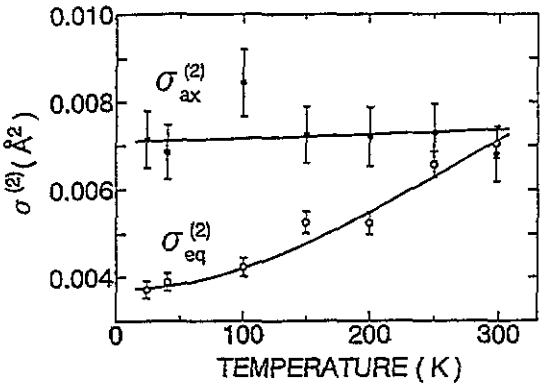

Figure 4. Temperature dependence of the Debye–Waller factors on the Ta–O atomic pair: ●, $\sigma^{(2)}_{ax}$ in the axial direction; ○, $\sigma^{(2)}_{eq}$ in the equatorial plane; ——, guide to the eye.

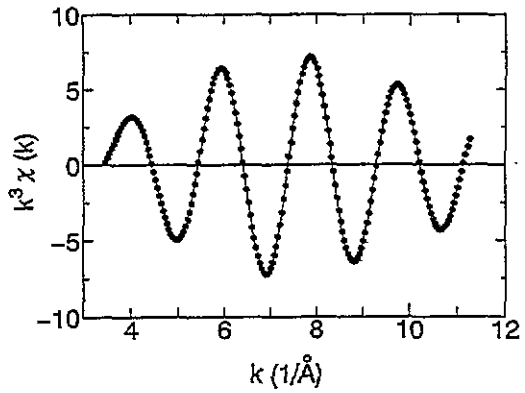

Figure 5. Comparison of an experimental EXAFS function $k^3\chi(k)$ of the first-nearest-neighbour O atom around the Ta atom (●) with a theoretical function (——).

As mentioned above, a Debye–Waller factor in an EXAFS function contains information on all modes of atomic vibration. The difference between the two σ-values corresponds to anisotropy of the thermal vibration of the Ta atom and increases with decreasing temperature. In the Slater mode, atomic vibration is triply degenerate in each axial direction. When we consider one of the triply degenerate vibrations from the viewpoint of local environment, we can imagine the atomic distribution of the Ta atom at the centre of the O octahedron, namely the ellipsoid of the probability density function has a long principal axis along the axial direction. Even though the Ta atom is displaced in either direction along the principal axes, the local structure around the Ta atom is equivalent to this probability density function so far as we observe it by the EXAFS technique. In any case, it is certain that this vibration of the Ta atom has cubic symmetry because of the triple degeneration of the phonon mode as long as the Ta atom is located at the centrosymmetric position. Anisotropy of atomic motion, where it is estimated by EXAFS analysis, will originate mainly from a large displacement due to the loss of the restoring force for the atomic motion by the softening of the phonon mode. At room temperature, the probability density function of the Ta atom is considered to be spherical or isotropic since the $\sigma^{(2)}_{ax}$ is not different from $\sigma^{(2)}_{eq}$ within the estimated standard

deviation. The temperature dependence of the difference between $\sigma_{ax}^{(2)}$ and $\sigma_{eq}^{(2)}$ implies that the probability density function of the Ta atom increases in the axial direction with decreasing temperature. The temperature dependence of the Debye–Waller factor for both optical and acoustic phonon modes calculated by Fujikawa and Miyanaga [32] is similar to our result for the Debye–Waller factors as shown in figure 4. In the strict sense, we should not compare with them because both $\sigma_{ax}^{(2)}$ and $\sigma_{eq}^{(2)}$ include contributions from optical and acoustic phonon modes. Strong anisotropy in the dispersion of a transverse acoustic phonon was found by Comes and Shirane [25]. However, an averaged atomic vibration is observed in spite of the anisotropic dispersion relation. The softening of the transverse optical phonon at $q = 0$ will contribute much to the anisotropy of thermal vibration of atoms estimated by EXAFS analysis. The phonon dispersion relation along the [001] direction shows that the transverse optical branch at $q = 0$ has a small value of phonon energy even at room temperature [23]. In fact, an anisotropic thermal vibration of the Ta atom may be expected at room temperature. However, it cannot be confirmed at room temperature as shown in figure 4, suggesting that the small anisotropy of the thermal vibration which originates from the softening of the transverse optical mode smears out and cannot be detected by the EXAFS analysis because the EXAFS signal is subject to contributions from all phonon modes.

The Debye–Waller factor $\sigma^{(2)}$ in the EXAFS function is expressed using the mean square displacement and the displacement correlation function as follows [35]:

$$\sigma^{(2)} = \langle(\hat{R}_{Ta-O} \cdot \delta u)^2\rangle \tag{6a}$$

$$= \langle(\hat{R}_{Ta-O} \cdot (u_{Ta} - u_O))^2\rangle \tag{6b}$$

$$= \langle(\hat{R}_{Ta-O} \cdot u_{Ta})^2\rangle + \langle(\hat{R}_{Ta-O} \cdot u_O)^2\rangle - 2\langle(\hat{R}_{Ta-O} \cdot u_{Ta})(\hat{R}_{Ta-O} \cdot u_O)\rangle \tag{6c}$$

where $\hat{R}_{Ta-O}$ is a unit vector, and u_{Ta} and u_O are the displacement vectors of the Ta and O atoms, respectively. Here we assumed that the anisotropic atomic motion originates from the softening of the Slater mode. We have substituted a single parameter u_S for these atomic displacements because u_S is proportional to u_{Ta} and $-u_O$, while u_e is an effective parameter due to other phonon modes having a normal temperature dependence and responsible for the isotropy. The difference between the Debye–Waller factors can be estimated in terms of means squares $\langle u_S^2\rangle$ and $\langle u_e^2\rangle$ of the atomic displacements:

$$\Delta\sigma^{(2)} = \sigma_{ax}^{(2)} - \sigma_{eq}^{(2)} \tag{7a}$$

$$= \langle u_S^2\rangle - \langle u_e^2\rangle. \tag{7b}$$

In the harmonic approximation, the mean square $\langle u^2\rangle$ of the atomic displacement is proportional to the sum of the square of the normal coordinate for the phonon of q in the sth branch Q_{qs}. A phonon mode in a crystal in thermal equilibrium has an energy given by

$$\tfrac{1}{2}\omega_{qs}^2\langle Q_{qs}Q_{qs}^*\rangle = \tfrac{1}{2}(\langle n_{qs}\rangle + \tfrac{1}{2})\hbar\omega_{qs} \tag{8}$$

where ω_{qs} is the phonon frequency for the transverse optical phonon and $\langle n_{qs}\rangle$ the thermal equilibrium occupancy of phonons. When the form of $\langle n_{qs}\rangle$ is given by the Planck distribution function, $\langle u^2\rangle$ can be calculated as a function of ω_{qs} and temperature T:

$$\langle u^2\rangle \propto \sum_{q,s} \frac{\hbar}{\omega_{qs}} \coth\left(\frac{\hbar\omega_{qs}}{2k_B T}\right) \tag{9}$$

where k_B is the Boltzmann constant. This equation is related to the expression for dielectric constant derived by Barrett [26]. The mean square $\langle u_S^2 \rangle$ of the atomic displacement due to the softening of the transverse optical mode at $q = 0$ was estimated from the data reported by Shirane *et al* [23] using equation (9). When estimating the effective term $\langle u_e^2 \rangle$ due to the other phonon mode, the phonon energy was assumed to be the same value at 295 K and considered to be constant below room temperature because an anisotropic vibration in this crystal cannot be detected at room temperature by the EXAFS analysis. Here the data above 40 K are taken from [23] because their crystal might have a phase transition at approximately 10 K probably owing to the impurity. The difference $\langle u_S^2 \rangle - \langle u_e^2 \rangle$ between the mean squares of the atomic displacement (open circles), which was normalized adequately, is compared with the difference $\Delta\sigma^{(2)}$ between the Debye–Waller factors (full circles) in figure 6. The agreement between the temperature dependences of these quantities is good. Here we did not adopt an anharmonic vibration model because the number of variables for the model is prevented from exceeding the number of degrees of freedom according to the information theory [36].

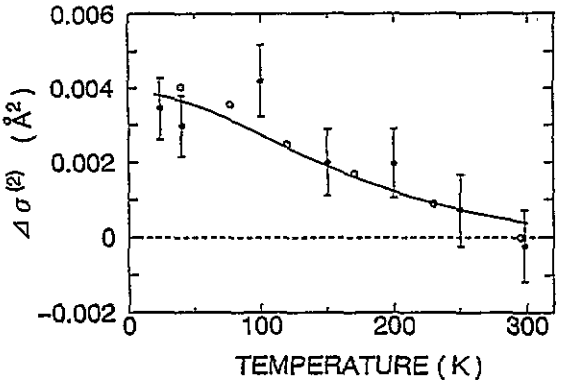

Figure 6. Comparison of the difference $\Delta\sigma^{(2)} = \sigma_{ax}^{(2)} - \sigma_{eq}^{(2)}$ between two Debye–Waller factors, estimated by the EXAFS analysis (●) with the difference between the mean squares of atomic displacement estimated by the data from inelastic neutron scattering (○).

The mean displacement of the Ta atom from the centre of the O octahedron at 298 K is estimated to be $u_{ax} = 0.082(4)$ Å in the axial direction. This is larger than $u_{ND} = 0.05(1)$ Å, which is estimated from neutron diffraction data [33]. This suggests that the Debye–Waller factor of the EXAFS function is emphasized by the thermal motion of the Ta and O atoms in the opposite phase.

We can conclude that the large Debye–Waller factors due to the atomic motion in the opposite phase at room temperature and the increase in anisotropic vibration of atoms at low temperatures are consistent with the strong linear-displacement correlation along the ⟨001⟩ directions and the softening of the transverse optical phonon at the Brillouin zone centre (Slater mode) from the viewpoint of the local environment around the Ta atom in $KTaO_3$.

5. Conclusion

The local structure around the Ta atom in $KTaO_3$ has been investigated from 24 to 298 K by the EXAFS technique. In the parameter fitting, we have introduced the technique of Fourier

filtering the theoretical EXAFS function twice under identical conditions with the data, so that we can discuss the Debye–Waller factors of EXAFS data. The one-shell models for the nearest-neighbour oxygen atoms have revealed that there is no marked local structure modification around the Ta atom. The interatomic distance R_{Ta-O}, and the mean free path of the photoelectron are found to be independent of temperature within the estimated standard deviations. The Debye–Waller factor $\sigma^{(2)}$ decreases monotonically with decreasing temperature. There is no component for anharmonic vibration of atoms, suggesting that the coupling of optical and acoustic phonon modes is important in order to understand the softening of the phonon mode. We can explain the local structure of $KTaO_3$ by leaving the Ta atom at the centre of the O octahedron and need not adopt the disorder model. The two-shell model shows that the temperature dependence of the Debye–Waller factor $\sigma_{ax}^{(2)}$ in the axial direction is different from the Debye–Waller factor $\sigma_{eq}^{(2)}$ in the equatorial plane. The anisotropy of the thermal vibration of the Ta atom increases with decreasing temperature. We have estimated the mean square displacement of atoms for both the transverse optical phonon and other phonons by making use of the phonon energy determined by an inelastic neutron scattering study. The temperature dependence of the anisotropic thermal motion estimated by the inelastic neutron scattering is successfully consistent with that estimated by the EXAFS analysis. This indicates that the local structure in $KTaO_3$ can be described by the concept of the soft phonon mode. Moreover, the Debye–Waller factor $\sigma_{ax}^{(2)}$ is evaluated as a large value by the EXAFS analysis, suggesting that relative atomic motion for the Ta and O atoms in the opposite phase is more dominant locally. The linear correlation of the atomic displacement along the ⟨001⟩ directions in $KTaO_3$ is also confirmed to be dynamical by the EXAFS technique.

Acknowledgments

The authors wish to thank J Zhuan and T Shimada for their assistance in the experiment at the Photon Factory. They are also indebted to Dr T Ishii for helpful discussion. They are grateful for the use of the diffractometer in the X-ray Laboratory of Okayama University. This work has been performed under a proposal of the Photon Factory Program Advisory Committee (proposal 91-187). This work was supported by the Okayama Foundation for Science and Technology and also supported by the Itoh Science Foundation.

References

[1] Cochran W 1960 *Adv. Phys.* 9 387
[2] Cowley R A 1962 *Phys. Rev. Lett.* 9 159
[3] Cowley R A 1964 *Phys. Rev.* **134** A981
[4] Yamada Y, Shirane G and Linz A 1969 *Phys. Rev.* **177** 848
[5] Shirane G and Yamada Y 1969 *Phys. Rev.* **177** 858
[6] Shirane G, Axe J D, Harada J and Remeika J P 1970 *Phys. Rev.* B **2** 155
[7] Shirane G, Axe J D, Harada J and Linz A 1970 *Phys. Rev.* B **2** 3651
[8] Harada J, Axe J D and Shirane G 1971 *Phys. Rev.* B **4** 155
[9] Shapiro S M, Axe J D, Shirane G and Riste T 1972 *Phys. Rev.* B **6** 4332
[10] Comes R, Denoyer F and Lambert M 1971 *J. Physique* **32** C5a 195
[11] Comes R, Lambert M and Guinier A 1968 *Solid State Commun.* **6** 715
[12] Comes P R, Lambert M and Guinier A 1970 *Acta Crystallogr.* A **26** 244
[13] Comes R, Denoyer F, Deschamps L and Lambert M 1971 *Phys. Lett.* **34A** 65
[14] Denoyer F, Comes R and Lambert M 1971 *Acta Crystallogr.* A **27** 414
[15] Itoh K, Zeng L Z, Nakamura E and Mishima N 1985 *Ferroelectrics* **63** 29

[16] Nelmes R J, Piltz R O, Kuhs W F, Tun Z and Restori R 1990 *Ferroelectrics* **108** 165
[17] de Mathan N, Prouzet E, Husson E and Dexpert H 1993 *J. Phys.: Condens. Matter* **5** 1261
[18] Ravel B, Stern E A, Yacobi Y and Dogan F 1993 *Japan. J. Appl. Phys.* **32** *Suppl.* **2** 782
[19] Abel W R 1971 *Phys. Rev.* B **4** 2696
[20] Samara G A and Morosin B *1973 Phys. Rev.* B **8** *1256*
[21] Lowndes R P and Rastogi A 1973 *J. Phys. C: Solid State Phys.* **6** 932
[22] Chaves A S, Barreto F C S and Ribeiro L A A 1976 *Phys. Rev. Lett.* **37** 618
[23] *Shirane G, Nathans R and Minkiewicz V J 1967 Phys. Rev.* **157** *396*
[24] Axe J D, Harada J and Shirane G 1970 *Phys. Rev.* B **1** 1227
[25] Comes R and Shirane G 1972 *Phys. Rev.* B **5** 1886
[26] Barrett J H 1952 *Phys. Rev.* **86** *118*
[27] Maeda H 1987 *J. Phys. Soc. Japan* **56** 2777
[28] Lytle F W, Sayers D E and Stern E A 1989 *Physica* B **158** 701
[29] Maeda H, Yoshiasa A, Koto K and Ishii T 1990 *Solid State Ion.* **40/41** 345
[30] Mckale A G, Veal B W, Paulikas A P, Chan S K and Knapp G S 1988 *J. Am. Chem. Soc.* **110** 3763
[31] Maeda H 1993 unpublished
[32] Miyanaga T and Fujikawa T 1994 *J. Phys. Soc. Japan* **63** 1036
[33] Harada J, Axe J D and Shirane G 1970 *Acta Crystallogr.* A **26** 608
[34] Ishii T 1992 *J. Phys.: Condens. Matter* **4** 8029
[35] Beni G and Platzman P M 1976 *Phys. Rev.* B **14** 1514
[36] Teo B K 1986 *EXAFS: Basic Principles and Data Analysis* (Berlin: Springer) p 132